International Core Journal of Engineering Volume 6 Issue 6, 2020
ISSN: 2414-1895 DOI: 10.6919/ICJE.202006_6(6).0042

Active Contours Driven by Local Image Difference Fitting Energy

Hongyan Zhang[a], Yongsheng Dong, Lintao Zheng, Lin Wang and Mingxin Jin

Henan University of Science and Technology, Luoyang 471000, China.

[a]hongyanzhang9@163.com

Abstract

A novel region-based active contour model (ACM) is proposed in this paper. By introducing the local image difference fitting (LIDF) energy to extract the local image difference information, our model is able to segment images with intensity inhomogeneities. Moreover, we utilize a Gaussian filtering method based on a Gaussian variational level set to smooth the level set function. It can not only ensure the smoothness of the level set function, but also eliminate the requirement of re-initialization, which is very computationally expensive. Experiments on images demonstrate the advantages of the proposed method over the state of art texture segmentation models in terms of both efficiency and accuracy.

Keywords

Image segmentation, Chan-Vese (C-V), Active contour models, Gaussian fifiltering.

1. Introduction

Image segmentation is one of the most crucial and challenging tasks in computer vision and pattern recognition, which is very helpful for object recognition, object detection, image retrieval, scene analysis, medical images processing, and video surveillance,etc. [1]. So far, a wide variety of methods have been proposed in this field including the region merging based methods [2,3], the graph based methods [4,5], and the active contour model (ACM) based methods [6], which could be found in several literatures [7-10]. Compared with the existing methods, the active contour models are able to achieve sub-pixel accuracy and provide a smooth and closed curve to represent the segmentation results, so it is widely used. The basic idea of the active contour models is to manage the evolving curve by minimizing the energy function.

ACM proposed by Kass [11] has been proved to be an efficient framework for image segmentation. As is well known, the original ACM framework has two obvious disadvantages: (1) it is sensitive to initial condition and (2) there are many difficulties associated with topology change of evolving contour. Later, people proposed many methods to improve the original ACM framework. Among them, the most successful and important one is the level set method, proposed by Osher and Sethian, which used a deformable curve front to detect the boundary of objects [12]. In the level set method,the curve is represented by the zero level set of a smooth function which is usually called the level set function.

After the work of Osher and Sethian [12], many variants of the level set model have been proposed. They could be divided into two categories, i.e., edge-based and region-based models. Generally, the edge-based models [13,14] segment images depend on the gradients information of images. However, merely using edge-based models is not easy to detect weak boundary. Region-based models aim to recognize each region of interest by using a certain region descriptor to guide the motion of the active contour. C-V model [15] is one of the most popular region-based models, which has been successfully used in binary phase segmentation with the assumption that each image region is statistically

ISSN: 2414-1895 DOI: 10.6919/ICJE.202006_6(6).0042

homogeneous. However, when for intensity inhomogeneity, the C-V model does not work well. Vese and Chan extended their work in [16] to utilize multiphase level set functions to represent multiple regions. Nonetheless, both the C-V and the extended models have the deficiency described above.

In order to segment images with intensity inhomogeneities, Min et al. [9] proposed a level set model for segmentation of natural image, which improved the convention C-V model and extracted the texture features by adaptive scale local variation degree algorithm. Furthermore, Dai et al. [17] proposed a method, which utilizes an inhomogeneity-embedded active contour as a segmentation model. And this method extracts inhomogeneous features for segmentation. To further improve performance, Gao et al. [18] proposed a model, which is called a factorization based active contours for texture segmentation.

In this paper, we propose a novel ACM model that can be used to segment images which are intensity inhomogeneities. We utilize the local image difference information to construct a local image difference fitting (LIDF) energy functional, which can be viewed as a constraint of the differences between the fitting image and the original image. Furthermore, we use Gaussian kernel filtering to regularize the level set function. In addition, re-initialization is not required in the proposed method. The analysis and experimental results show that the proposed method is more efficient than most of other current ACM models, and the effect is better.

The rest of this paper is organized as follows: In Section 2, we introduce the level set method of ACM firstly, then we review some classic active contour models and indicate its limitations. Section 3 describes our model and its variational formulation. Section 4 reports the experimental results. A conclusion is made in section 5.

2. Related Work

2.1 Level Set Method of ACM

Active contour model (ACM) is an iterative model for image segmentation, whose basic idea is to make the initial curve evolve under the interaction of a series of external constraints and the internal energy of the image until it satisfies a certain convergence condition, it will stop at the edges of the image and realize the image segmentation. Compared with other segmentation models, there are two main advantages ACMs have: (1) In ACMs, the segmentation result of given image is encircled by closed and smooth curve, which is able to perfectly describe the object boundary and obtain sub-pixel segmentation accuracy. (2) Generally, due to the evolving curve is implicitly expressed through level set function, making ACMs numerially stable during the iteration. In addition, the topological changes of objects to be segmented can be achieved. For the level set image processing method, it directly forms a general algorithm: Set the initial state of the level set function. And determine the form of the power. Then derive the states of the level set function according to the basic equations. At last, solve a zero level set for the state of each level set function. Then it can be seen that after several iterations, the object in the given image is enclosed by the closed and smooth curve.

ACM method mainly uses the gradient information of the image. For a relatively noisy or blurred image, this method is difficult to be effective, and even an incorrect segmentation result may occur.

Up to now there have been a large number of published active contour models. These models are based on curve evolution theory and level set method . The basic idea is to represent contours as the zero level set of an implicit function defined in a higher dimension, usually referred as the level set function, and to evolve the level set function according to a partial differential equation(PDE).

2.2 the Mumford and Shah (MS) Model

Mumford and Shah [19] formulated the image segmentation problem as follows: find an optimal piecewise smooth approximation function u of image I, which varies smoothly within each sub-region Ωi of image domain $\Omega \subset R2$, and rapidly or discontinuously goes across the boundaries of Ωi. They proposed the following energy functional:

ISSN: 2414-1895 DOI: 10.6919/ICJE.202006_6(6).0042

$$E^{MS}(u,C)=\int_{\Omega}(u-I)^2dx+\mu\int_{\Omega/C}|\nabla u|^2dx+\nu|C|,\quad x\in\Omega, \tag{1}$$

where |C| is the length of the contour C, μ, ν > 0 are fixed positive parameters.

The non-convexity of the unknown set C and the above energy function makes it difficult to minimize. Therefore, some alternative methods have been proposed to simplify or modify the above functional.

2.3 Chan-Vese (C-V) Model

Chan and Vese [15] proposed an ACM which can be seen as a special case of the Munford-Shah problem [19]. For a given image I, the C-V model is formulated by minimizing the following energy functional:

$$E^{CV}=\lambda_1\int_{inside(C)}|I(x)-c_1|^2dx+\lambda_2\int_{outside(C)}|I(x)-c_2|^2dx,\quad x\in\Omega, \tag{2}$$

where c1 and c2 are two constants which are the average intensities inside and outside the contour, respectively.

In traditional level set methods, the evolving curve C in Ω is defined as the zero level set function $\{(x, y) \in \Omega \mid \phi(x, y) = 0\}$. Figure 1 shows a diagram of ϕ, it can be found that the region inside the red circle is greater than zero and the region outside the red circle is smaller than zero. We replace the unknown variable C by the unknown variable ϕ. The C-V model utilizes this level set formulation to solve the evolving curve C .

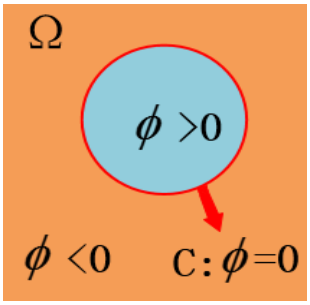

Figure 1. The example of the level set method: the implicit representation of C (red circle) on domain Ω, which is divided into two regions according to ϕ

By minimizing Eq. (1), c1 and c2 are computed by:

$$c_1(\phi)=\frac{\int_{\Omega}I(x)\cdot H(\phi)dx}{\int_{\Omega}H(\phi)dx}, \tag{3}$$

$$c_2(\phi)=\frac{\int_{\Omega}I(x)\cdot(1-H(\phi))dx}{\int_{\Omega}(1-H(\phi))dx}, \tag{4}$$

where H(ϕ) is the Heaviside function and δ(ϕ) is the Dirac function. Generally, choose the regularized versions as follows:

$$H_{\varepsilon}(z)=\frac{1}{2}(1+\frac{2}{\pi}\arctan(\frac{z}{\varepsilon})), \tag{5}$$

$$\delta_{\varepsilon}(z)=\frac{1}{\pi}\cdot\frac{\varepsilon}{\varepsilon^2+z^2},\qquad z\in R, \tag{6}$$

If ε is too small, the values of δε(z) tend to be near zero to make its effective range small (see Figure 2), so the energy functional has a tendency to fall into a local minimum. The object may fail to be extracted if the initial contour starts far from it. However, if ε is large, although δε(z) tends to obtain a global minimum, the finial contour location may not be accurate [20].

ISSN: 2414-1895 DOI: 10.6919/ICJE.202006_6(6).0042

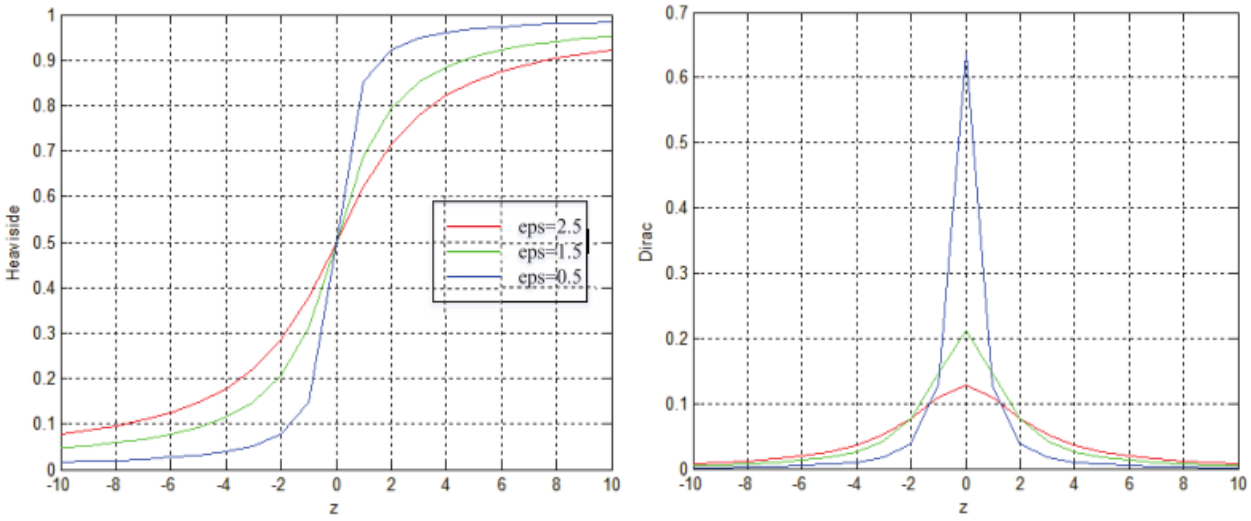

Figure 2. Graphs of Heaviside and Dirac function

By incorporating the length and area energy terms into Eq. (2) and minimizing them, the corresponding level set formulation can be computed by:

$$\frac{\partial \phi}{\partial t} = \delta(\phi)\left[\mu\nabla\left(\frac{\nabla\phi}{|\nabla\phi|}\right) - \nu - \lambda_1(I-c_1)^2 + \lambda_2(I-c_2)^2\right], \tag{7}$$

where $\mu \geq 0$, $\nu \geq 0$, $\lambda 1 > 0$, $\lambda 2 > 0$ are fixed parameters, μ controls the smoothness of zero level set, ν increases the propagation speed, and $\lambda 1$ and $\lambda 2$ control the image data driven force inside and outside the contour, respectively. ∇ is the gradient operator. The C-V model is a classic method. But when the image intensity inside or outside the contour is inhomogeneous, C-V model is not applicable.

2.4 the Piecewise Smooth (PS) Model

Although the C-V model is classic, it does not work well for the images with intensity inhomogeneities. Chan and Vese proposed another way to solve this problem in [16], expressing the intensity inside and outside the contour as a piecewise smoothing function rather than a constant. They defined the following energy functional:

$$\begin{aligned} E^{PS}(u^+,u^-,\phi) &= \int_\Omega |u^+ - I|^2 H(\phi)dx + \int_\Omega |u^- - I|^2 (1-H(\phi))dx \\ &+ \mu\int_\Omega |\nabla u^+|^2 H(\phi)dx + \int_\Omega |\nabla u^-|^2 (1-H(\phi))dx + \nu\int_\Omega |\nabla H(\phi)|, \quad x \in \Omega, \end{aligned} \tag{8}$$

where $\mu, \nu \geq 0$ are fixed parameters, $I : \Omega \rightarrow R$ denotes the original image, u+(x) and u-(x) are smooth functions in the sub-regions $\Omega+ = \{x \in \Omega : \phi(x) > 0\}$ and $\Omega- = \{x \in \Omega : \phi(x) < 0\}$, respectively. We minimize the above energy functional and get the following EulerCLagrange equations:

$$\frac{\partial \phi}{\partial t} = \delta(\phi)\left[\nu div\left(\frac{\nabla\phi}{|\nabla\phi|}\right) - |u^+ - I|^2 - \mu|\nabla u^+|^2 + |u^- - I|^2 + \mu|\nabla u^-|^2\right], \tag{9}$$

Obviously, in the implementation of PS model, the computational cost of acquiring u+ and u- is high and must be extended to the entire image domain, which is difficult to achieve. In summary, high complexity limits the application of the PS model in practice.

ISSN: 2414-1895 DOI: 10.6919/ICJE.202006_6(6).0042

3. Proposed Method

3.1 LIDF Model and Its Variational Level Set Formulation

In this paper, we propose a local image difference fitting (LIDF) formulation which is defined as follows:

$$P=\left(m_1-\frac{c_1}{2}\right)H_\varepsilon(\phi)+\left(m_2-\frac{c_2}{2}\right)(1-H_\varepsilon(\phi)), \tag{10}$$

where c1 and c2 are defined in Eqs. (2) and (3), m1 and m2 [21] are computed by:

$$m_1=\frac{(I(x)\cdot H(\phi))*K_\sigma(x)}{H(\phi)*K_\sigma(x)} \tag{11}$$

$$m_2=\frac{(I(x)\cdot(1-H(\phi)))*K_\sigma(x)}{(1-H(\phi))*K_\sigma(x)} \tag{12}$$

where $*$ donotes two-dimensional convolution operation. And we choose a truncated Gaussian window Kσ(x) with standard deviations and of size 4k+1 by 4k+1, where k is the greatest integer smaller than σ. Similar segmentation results can be achieved if we choose a constant window.

Based on Eq. (10) , we propose a local image difference fitting (LIDF) energy functional by minimizing the difference between the fitted difference image and the original image. The level set formulation is as follows:

$$E_P(\phi)=\frac{1}{2}\int_\Omega |I(x)-P(x)|^2 dx, \qquad x\in\Omega \tag{13}$$

To maintain the regularity of the level set function during the evolution process of active contour, we introduce a level set regularization term proposed by Li et al. [2] in our level set formulation, which is defined as:

$$E_R(\phi)=\int_\Omega \frac{1}{2}(|\nabla\phi(x)-1|)^2 dx \tag{14}$$

where $\nabla\phi$ denotes the derivate of the level set function. Therefore, the energy functional proposed by this article is represented as follows:

$$E(\phi)=\mu E_P(\phi)+\nu E_R(\phi) \tag{15}$$

where μ and ν are two positive constants, used to balance the proportion of the total energy with respect to their corresponding terms.

Using the gradient descend method, we minimize the energy functional E(ϕ) with respect to ϕ to get the corresponding gradient descent flow (please refer to Appendix A for detailed derivation):

$$\frac{\partial\phi}{\partial t}=-\frac{\partial E(\phi)}{\partial\phi}=\mu(I-P)\left(m_1-m_2+\frac{c_2-c_1}{2}\right)\delta_\varepsilon(\phi)+\nu\left(\nabla^2\phi-div\left(\frac{\nabla\phi}{|\nabla\phi|}\right)\right) \tag{16}$$

where δε(φ) is the Dirac function defined in Eq. (6). And thus the updating procedure of level set function is defined as:

$$\phi_{t+1}=\phi_t+\frac{\partial\phi}{\partial t}\Delta t \tag{17}$$

3.2 Algorithm Summarization

In the traditional level set methods, the level set function is initialized to be an SDF to its interface in order to prevent it from being too steep or flat near its interface, and re-initialization is required in the evolution. However, removing the zero level set away from the interface has an adverse side effect. In addition, it is difficult to determine when and how to apply re-initialization. In addition, re-

ISSN: 2414-1895 DOI: 10.6919/ICJE.202006_6(6).0042

initialization is a very expensive operation. In order to solve this problem, we introduce a level set regularization term proposed by Li et al. [2]. In addition, we utilize a Gaussian kernel to regularize the selective binary level set function after each iteration. In our method, the level set function is initialized into a constant in order to achieve simplicity in practice.

The main computing steps of the algorithm can be summarized as follows:

Step 1: Initialize the level set function φ to be a binary function as follows:

$$\phi = \begin{cases} -\rho, & x \in \Omega - \partial\Omega_0 \\ 0, & x \in \partial\Omega_0 \\ \rho, & x \in \Omega - \Omega_0 \end{cases} \tag{18}$$

where ρ > 0 is a constant, Ω0 is a subset in the image domain Ω, and ∂Ω0 is the boundary of Ω0.

Step 2: Solve c1, c2, m1 and m2 by Eq. (2), (3), (11) and (12) respectively.

Step 3: Evolve the level set function ϕ according to Eq. (16).

Step 4: Smooth the level set function by a Gaussian kernel, i.e. $\phi = G\varsigma * \phi$, where ς is the standard deviation, which should be larger than the aquare root of the time-step Δt in order to enhance the smoothing capacity.

Step 5: Check whether the evolution is stable. If not, t=t+1 and return to step 2.

3.3 Advantage of Our Model Over the C-V Model

In contrast to the C-V model, our model utilizes the image statistical information to stop the curve evolution on the desired boundaries, so it is robust to noise. Furthermore, our model can well handle images with weak edges or without edges. In addition, our model can selectively extract the desired object by setting the initial contour surrounding the desired boundaries, while the C-V model will extract all the objects. Therefore, the segmentation results obtained by C-V model will be very unsatisfactory (see Figure 3 in Section IV for example). Furthermore, the evolution direction in our model can be controlled to obtain satisfying segmentation results, while the CCV model may get disordered results (see Figure 3 in Section IV for example). Finally, our model has less computational complexity than the C-V model.

4. Experiments

Our algorithm is implemented in Matlab R2014a on a 3.4- GHz Intel Founder personal computer. In this section, we test the effectiveness of our proposed method on several synthetic and inhomogeneous nature images, and in our experiment, we set μ is 1, ν is 1, and set the same parameters ρ = 1, ε = 1, ς = 0.45. In addition, time-step Δt is set to 1. The value of parameter σ is chosen by experience according to the images.

4.1 Experimental Results and Analysis of Synthetic Images

In the first experiment, we compared the segmentation performance of the traditional C-V method [15] and our proposed LIDF active contour segmentation algorithm. It can be seen from the figure that the initial contour map is displayed in the first column of Figure 3. The second column shows the segmentation results of the CV model. However, the third column in the figure shows that our method can accurately extract all objects and locate object boundaries. In addition, we will apply the proposed method to two different types of synthetic texture images, including normal texture images and texture images with uneven illumination (as shown in Figure 4). In addition, our model is compared with existing texture segmentation technologies such as C-V [15] model, local contour-based active contour model (LSACM) [22] and factorization-based interactive contour segmentation model (FBM) [23].

ISSN: 2414-1895 DOI: 10.6919/ICJE.202006_6(6).0042

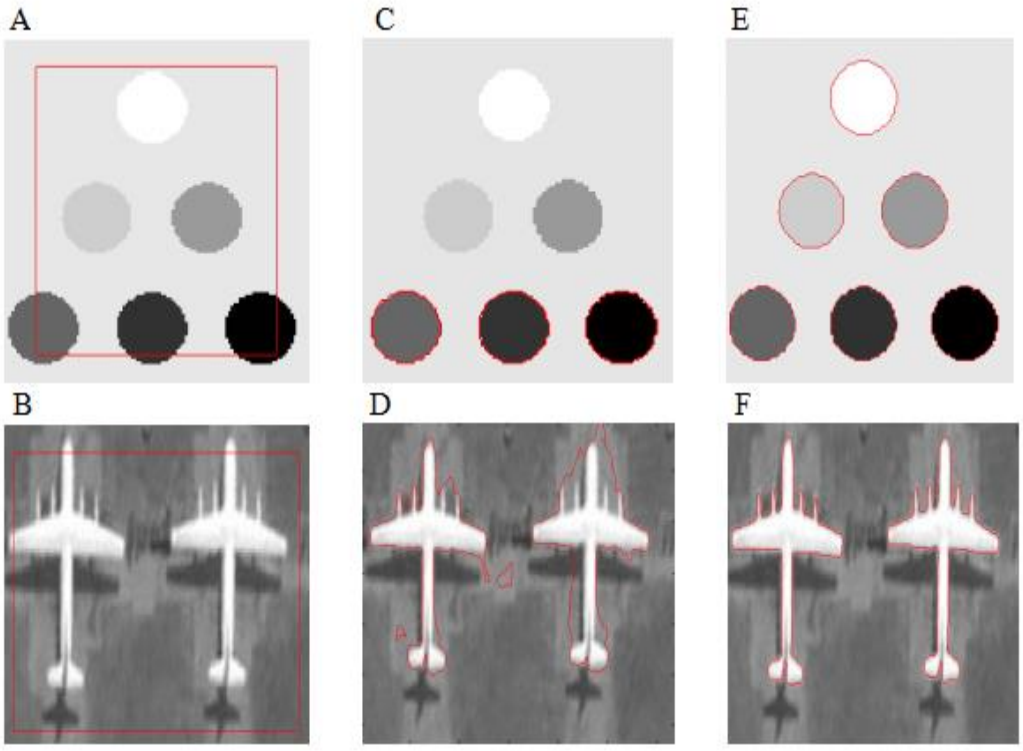

Figure 3. Comparisons of the global segmentation property between the C-V model and the proposed method. The left column shows the initial contours, the middle and right columns show the corresponding segmentation results of C-V model and proposed method

Table 1. Iteration CPU time and segmentation accuracy of C-V model and our LIDF model

	Figure 3(A)			Figure 3(B)		
	252×252 pixels			252×252 pixels		
	iterations	time(s)	SA (%)	iterations	time(s)	SA (%)
C-V	80	7.53	47.44	120	8.42	72.25
LIDF	20	5.42	97.32	85	6.37	98.79

In Figure 4, we experiment on image G and image H. In the Figure 4, column (a) is the initial contour map of the two images, column (b) is the standard manual segmentation result as a reference standard, column (c) is the segmentation result of the CV model, and (d) is the LSACM algorithm The result of segmentation, column (e) is the segmentation result of FBM algorithm, column (f) is the segmentation result of our proposed method. It can be seen from Figure 3-4, our LIDF segmentation model is better than C-V model, LSACM algorithm and FBM algorithm. The segmentation result of FBM algorithm is close to the result of manual segmentation, however, the LIDF model we proposed is more perfect than it. Based on Figure 3-4, it can be seen that the LIDF model can provide the desired results in the composite image and can more accurately locate the object boundary.

The converged iterations, CPU time and segmentation accuracy for specific size images in Figure 3 are compared in Table 1. It shows that our method is faster than C-V model, and the number of iterations by ours is fewer than that by C-V model. In addition, the accuracy of the segmentation is also higher. So our method is more efficient and more accurate.

ISSN: 2414-1895 DOI: 10.6919/ICJE.202006_6(6).0042

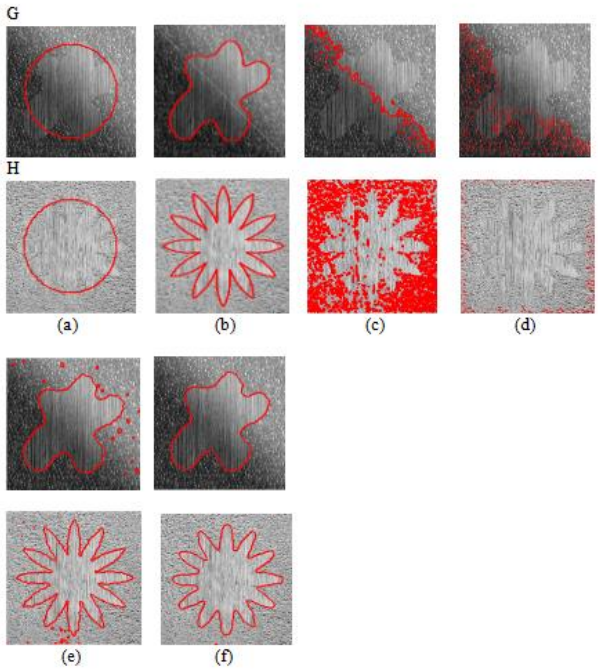

Figure 4. Segmentation results on synthetic images. The first row of (a): normal texture image; the second row of (a): texture image with illumination inhomogeneous. (b) ground truth, (c) C-V, (d) LSACM, (e) FBM, (f) LIDF

Table 2 shows the accuracy obtained by comparing the segmentation results of several methods in Figure 4 with the ground truth, where the similarity measure is provided by [24].

Table 2. The segmentation accuracy between our model and other methods

Image	C-V	LSACM	FBM	Proposed
G	0.501	0.421	0.919	**0.984**
H	0.528	0.021	0.938	**0.979**

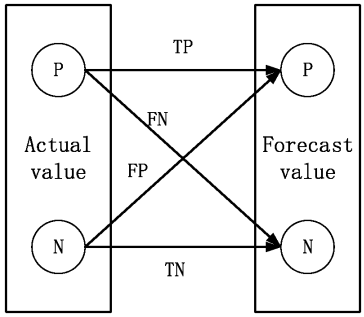

Figure 5. Relationship and connection between TP、TN、FP and FN

Regarding the segmentation accuracy SA, we must first understand several evaluation indicators, namely FP, FN, TP, and TN. P and N respectively represents the evaluation result of the algorithm, while F and T represent whether the result is correct. As shown in Figure 5, the judgment process of these four evaluation indicators is presented more clearly. Then SA is:

$$SA = \frac{TP + TN}{TP + TN + FP + FN} \tag{19}$$

4.2 Experimental Results and Analysis of Natural Images

In order to further highlight the advantages of our proposed LIDF model, in this section, we will conduct experiments on natural images to further verify the effectiveness of the algorithm.

ISSN: 2414-1895 DOI: 10.6919/ICJE.202006_6(6).0042

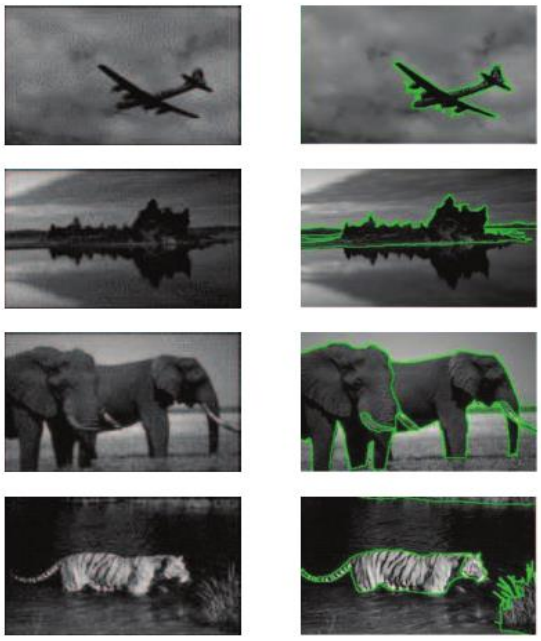

Figure 6. Segmentation results of our proposed method

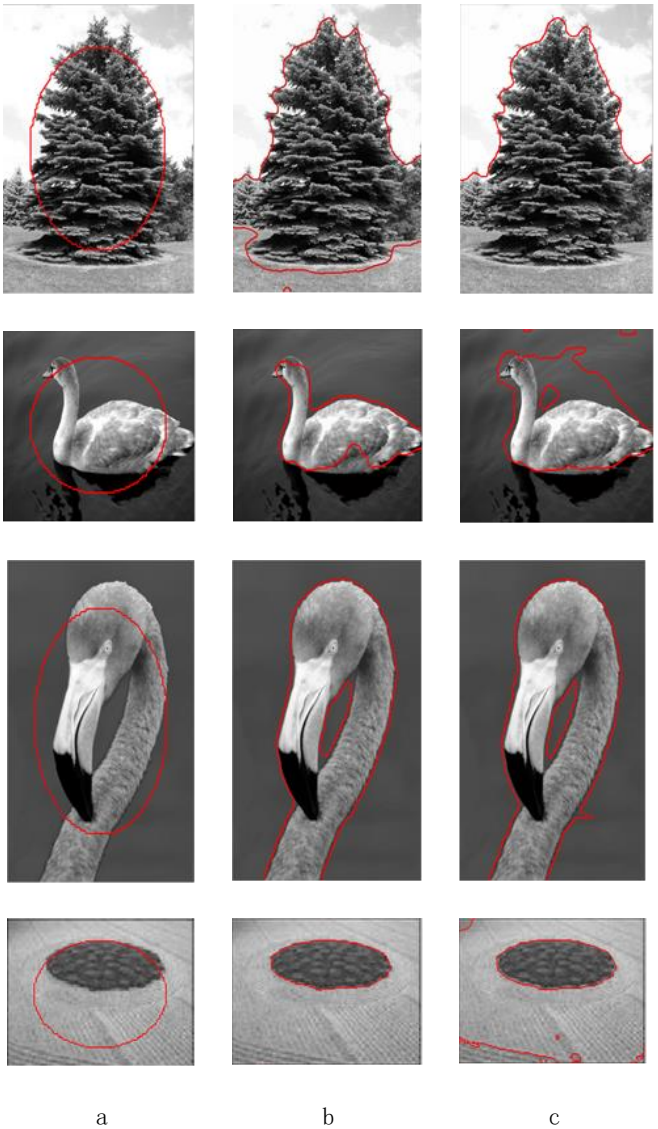

Figure 7. Comparison segmentation results between FBM method and the proposed method

ISSN: 2414-1895 DOI: 10.6919/ICJE.202006_6(6).0042

Figure 6 shows segmentation results of our method in some natural images that are more complex, such as objects with less obvious background, multiple objects, and more complex image textures. The left column shows the original images. The right columns show the segmentation results of the proposed method. It can be seen that our method can still segment these complex images well.

Figure 7 compares the performance of the FBM method and our method in segmenting natural images. Figure 7a shows the original images with initial contours. Figure 7b shows the segmentation results by our method. Figure 7c shows the corresponding segmentation results by FBM method. It can be seen that the our proposed method can more accurately locate the boundary of the object and get the desired object. The FBM method yields results similar to ours, but produces over-segmentation.

5. Conclusion

In this paper, we propose a novel active contour model driven by local image difference fifitting (LIDF) energy. The proposed LIDF energy functional has less computational complexity than the C-V energy functional. A novel level set method based on Gaussian fifiltering is used to implement our variational formulation, and the experimental results reveal that it is not only robust to prevent the energy functional from being trapped into local minimum, but also capable of keeping the level set function regular. Experiments demonstrate that our method can achieve satisfying segmentation results as the C-V model, and outperforms other methods in terms of both effificiency and accuracy.

References

[1] L. K. Lee, S. C. Liew, and W. J. Thong, “A review of image segmentation methodologies in medical image,” Lecture Notes in Electrical Engineering, pp. 1069-1080, 2015.

[2] C. Li, C. Xu, and C. Gui “Level set evolution without re-initialization: a new variational formulation,” IEEE Computer Society Conference on Computer Vision and Pattern Recognition, vol. 1, pp. 430-436, 2005.

[3] S. Qian, G. Weng, “Medical image segmentation based on FCM and level set algorithm,” IEEE International Conference on Software Engineering and Service Science, pp. 225-228, 2016.

[4] Y. Boykov, V. Kolmogorov, “An experimental comparison of min-cut/max-flow algorithms for energy minimization in vision,” IEEE Transactions on Pattern Analysis and Machine Intelligence,vol. 26, no. 9, pp. 1124-1137, 2004.

[5] S. Bao, P. Wang, and T. Mok, “3D randomized connection network with graph-based label inference,” IEEE Transactions on Image Processing, vol. 27, no. 8, pp. 3883-3892, 2018.

[6] H. Min, W. Jia, Y. Zhao, W. Zuo, and H. Ling, “Late: a level-set method based on local approximation of taylor expansion for segmenting intensity inhomogeneous images,” IEEE Transactions on Image Processing, vol. 27, no. 10, pp. 5016-5031, 2018.

[7] A. Khadidos, L. Zhang, and V. Sanchez, “Weighted level set evolution based on local edge features for medical image segmentation,” IEEE Transactions on Image Processing, vol. 26, no. 4, pp. 1979-1991, 2017.

[8] M. Gao, H. Chen, “Texture image segmentation using fused features and active contour,” IEEE International Conference on Pattern Recognition, pp. 2036-2041, 2017.

[9] H. Min, W. Jia, and X. Wang, “An Intensity-Texture model based level set method for image segmentation,” Pattern Recognition, vol. 48, no. 4, pp. 1547-1562, 2015.

[10] B. Peng, L. Zhang, and D. Zhang, “A survey of graph theoretical approaches to image segmentation,” Pattern Recognition, vol. 46, no. 3, pp. 1020-1038, 2013.

[11] M. Kass, A. Witkin, and D. Terzopoulos, “Snakes: active contour models,” Computer Vision and Image Understanding, vol. 77, no. 3, pp. 317-370, 2000.

[12] S. Osherand and J. Sethian, “Fronts propagating with curvaturedependent speed: algorithms based on Hamilton Jacobi formulations,” International Journal of Computer Physics, vol. 79, no. 1, pp. 12-49, 1998.

[13] V. Caselles, R. Kimmel, and G. Sapiro, “Geodesic active contours,” International Journal of Computer vision, vol. 22, no. 1, pp. 61-79, 1997.

ISSN: 2414-1895 DOI: 10.6919/ICJE.202006_6(6).0042

[14] R. Malladi, J. Sethian, and B. Vemuri, "Shape modeling with front propagation: a level set approach," IEEE Transactions on Pattern Analysis and Machine Intelligence, vol. 17, no. 2, pp. 158-175, 1995.

[15] T. Chan and L. Vese, "Active contour without edges," IEEE Transactions on Image Processing, vol. 10, no. 2, pp. 266-277, 2001.

[16] T. Chan and L. Vese, "A multiphase level set framework for image segmentation using the MumfordCShah model," International Journal of Computer Vision, vol. 50, no. 3, pp. 271-293, 2002.

[17] L. Dai, J. Ding, and J. Yang, "Inhomogeneity-embedded active contour for natural image segmentation," Pattern Recognition, vol. 48, no. 8, pp. 2513-2529, 2015.

[18] M. Gao, H. Chen, B. Fang, and S. Zheng, "A factorization based active contour model for texture segmentation," IEEE International Conference on Image Processing, pp. 4309-4313, 2016.

[19] D. Mumford and J. Shah, "Optimal approximation by piecewise smooth function and associated variational problems," Communication on Pure and Applied Mathematics, vol. 42, no. 5, pp. 577-685, 1989.

[20] C. Li, C. Kao, J. Gore, and Z. Ding, "Minimization of region-scalable fitting energy for image segmentation," IEEE Transactions on Image Processing, vol. 10, no. 17, pp. 1940-1949, 2008.

[21] C. Li and C. Kao, "Implicit active contour driven by local binary fitting energy," International Conference on Computer Vision and Pattern Recognition, pp. 1-7, 2007.

[22] K. Zhang, L. Zhang, and D. Zhang, "A level set approach to image segmentation with intensity inhomogeneity," IEEE Transactions on Cybernetics, vol. 46, no. 2, pp. 546-557, 2016.

[23] J. Yuan, D. Wang, and A. Cheriyadat, "Factorization-based texture segmentation," IEEE Transactions on Image Processing, vol. 24, no. 11, pp. 3488-3497, 2015.

[24] H. Chang, A. Zhuang, and D. Valentino, "Performance measure characterization for evaluating neuroimage segmentation algorithms," Neuroimage, vol. 47, no. 1, pp. 122-135, 2009.